Intramolecular excimers and energy migration in polyesters with 2,6-naphthalene dicarboxylic acid units separated by spacers of 1–4 ethylene oxide units

J. Gallego, F. Mendicuti and E. Saiz
Departamento de Química Física, Universidad de Alcalá de Henares, Alcalá de Henares, 28871 Madrid, Spain

and Wayne L. Mattice*
Institute of Polymer Science, The University of Akron, Akron, OH 44325-3909, USA
(Received 10 August 1992)

The fluorescence has been measured in dilute solution and in glassy poly(methyl methacrylate) for polyesters of 2,6-naphthalene dicarboxylate and HO–$(CH_2CH_2O)_m$–H, $m=1-4$. The model compounds in which the glycol connects two molecules of 2-naphthoate were also studied. Intramolecular energy migration is implied by the anisotropy of the fluorescence in rigid media. The results are consistent with Förster radii of about 12 Å in the model compounds and 14 Å in the polymers, as found previously for a similar series based on HO–$(CH_2)_m$–OH instead of HO–$(CH_2CH_2O)_m$–H.

(Keywords: anisotropy; energy migration; excimer; fluorescence; polyesters)

INTRODUCTION

Polymers containing naphthalene can form an intramolecular excimer either by direct excitation of one of the chromophores that forms the excited state dimer or by initial excitation of some other chromophore, followed by migration of the excitation until it is trapped[1]. Here we study both phenomena in the series of polyesters from 2,6-naphthalene dicarboxylic acid and four linear glycols, HO–$(CH_2CH_2O)_m$–H, $m=1-4$. Excimer formation is determined from the steady-state emission spectra, and the importance of energy migration is inferred from the anisotropy of the fluorescence when the polymers are dispersed in a rigid medium. The polymers are abbreviated P_m. We also study the bichromophoric model compounds, denoted NmN, that contain two naphthoyl units separated by m oxyethylene units, and the model compound 2-methylnaphthoate, denoted 2MN. Illustrative structures are depicted in *Figure 1*.

A rotational isomeric state treatment is employed for rationalization of the experimental results, namely, the dependence of I_D/I_M on m in NmN and the dependence of r_a on m in P_m. Here I_D/I_M denotes the ratio of the intensities of excimer and monomer emission and r_a is the anisotropy of the fluorescence. The values of the Förster radii[2] extracted from the data for the polymers with oxyethylene spacers are consistent with results reported for a similar series of polymers with methylene spacers[3].

* To whom correspondence should be addressed

EXPERIMENTAL

The synthesis and purification of the samples of P_m and NmN was performed starting from 2,6-naphthalene dicarboxylic acid chloride and HO–$(CH_2CH_2O)_m$–H by the same methods as those described previously for the P_m and NmN in which the glycol was HO–$(CH_2)_m$–OH[3]. Samples were characterized by n.m.r.

The solvents, 1,2-dichloroethane, methanol, ethylene glycol and propanol, were spectrophotometric or HPLC grade from Aldrich. Methyl methacrylate from Merck (>99%, stabilized with hydroquinone) was distilled under vacuum before use in the preparation of vitrified samples. These samples were prepared in poly(methyl methacrylate) in the manner described previously[3,4],

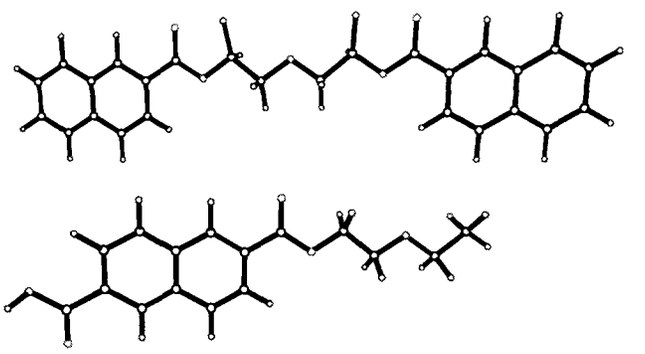

Figure 1 N2N (top) and a repeating unit of P2 (bottom), both in the all-*trans* conformation

0032-3861/93/122475-06

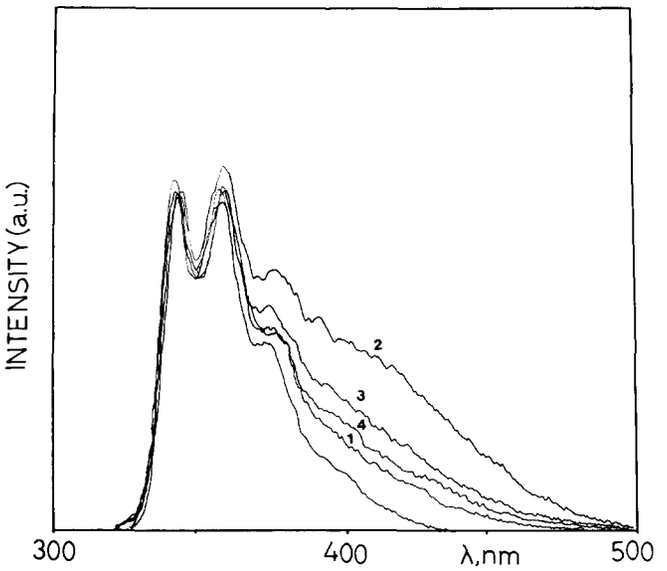

Figure 2 Emission spectra for 2MN and NmN, $m=1-4$, in methyl methacrylate at 25°C. Spectra are normalized at 342 nm, excitation is at 294 nm. The unlabelled spectrum is for 2MN and the labelled spectra are for the NmN with the indicated values of m

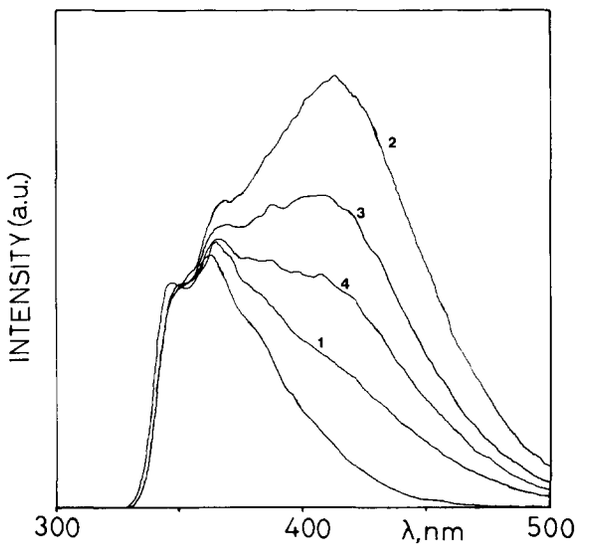

Figure 3 Emission spectra for 2MN and NmN, $m=1-4$, in propanol at 25°C. Spectra are normalized at 350 nm, excitation is at 294 nm. The unlabelled spectrum is for 2MN and the labelled spectra are for NmN with the indicated values of m

starting from solutions in methyl methacrylate that had an optical density of 0.5–1.0 at the wavelength of excitation (294 nm for NmN, 296 nm for P_m).

Most fluorescence measurements were performed at 25°C with a Perkin–Elmer LS-5B fluorimeter, using single monochromators in the excitation and emission paths. Slits were 15 nm for excitation and 2.5 or 5 nm for emission of samples in dilute solution and in vitrified glass, respectively. Magic angle conditions were employed for measurements in solution. Additional measurements of the anisotropy of the fluorescence for vitrified samples in poly(methyl methacrylate) were performed with an SLM 8000C equipped with a double monochromator in the excitation path and a single monochromator in the emission path. Slits with this instrument were 8 nm for both excitation and emission. Right-angle geometry was used for measurements in solution and front-face illumination (at 30° in the Perkin-Elmer and 35° in the SLM) was used for measurements with vitrified samples dispersed in poly(methyl methacrylate).

Solvent baselines were subtracted from the spectra. Excitation spectra and absorption spectra are similar to those reported for the series in which the glycol was $HO-(CH_2)_m-OH$[3]. The shapes of the excitation spectra do not depend on the choice of wavelength for monitoring the emission.

EMISSION SPECTRA

Figures 2 and *3* depict emission spectra in methyl methacrylate and in propanol, respectively, at 25°C for 2MN and the four NmN, $m=1-4$. Spectra are normalized at the peak of highest energy, which is observed at 345 and 350 nm in methyl methacrylate and propanol, respectively. Spectra obtained in methanol and ethylene glycol were normalized at 367 and 372 nm, respectively, because the separate peak seen at ~350 nm in the other two solvents is reduced to a small shoulder.

The enhanced intensity of NmN to the red of the emission from 2MN is attributed to the intramolecular formation of an excimer. Comparison of the spectra is facilitated by the use of I_D/I_M, defined here as[3]

$$I_D/I_M=(I_{NmN,400}-I_{2MN,400})/I_{norm} \quad (1)$$

where the intensities in the numerator are evaluated at 400 nm and the intensity in the denominator is evaluated at the wavelength chosen for normalization. A similar definition will be used for the P_m, using spectra of the type illustrated in *Figures 4* and *5*. Results are collected in *Table 1*. The trends of I_D/I_M with m in fluid solution are similar to those reported previously[5], with a maximum at $m=2$. The values of I_D/I_M in the vitrified samples are smaller than those in any of the fluid solutions. For spacers of a specified size, the value of I_D/I_M is larger for P_m than for NmN. This result suggests there is a mechanism for populating the excimer in P_m that is not accessible in NmN. Energy migration is an example of such a mechanism.

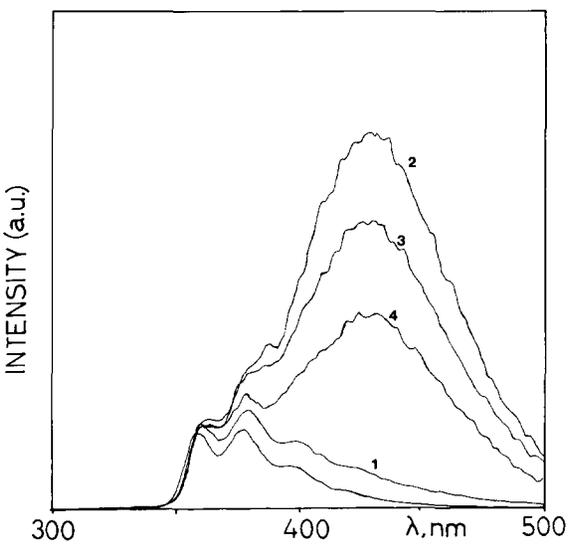

Figure 4 Emission spectra, normalized at 360 nm, for DMN and P_m, $m=1-4$, in methyl methacrylate at 25°C, using excitation at 296 nm. The unlabelled spectrum is for DMN and the labelled spectra are for P_m with the indicated values of m

ANISOTROPY OF THE FLUORESCENCE

The anisotropy of the fluorescence, denoted by r_a, was measured as described by Lakowicz[6], as done previously for the series where the flexible spacer was $HO-(CH_2)_m-OH$[3]. The largest values of r_a are obtained with two molecules, 2MN and DMN, that contain a single chromophore, as shown in *Table 2*. The value of r_a for DMN is in excellent agreement with the expectation of 0.4 for a random orientation of independent chromophores that do not rotate on the time scale of the fluorescence lifetime. Smaller values of r_a are obtained for molecules that contain more than one chromophore. When the size of the spacer is constant, the value of r_a decreases when more chromophores are incorporated into the chain (compare N*m*N and P_m at constant *m*). Within the series N*m*N, r_a increases as the size of the spacer increases, as it does also in the series P_m. These results suggest a higher efficiency of energy migration as the size of the spacer decreases.

THEORETICAL INTERPRETATION

The bond lengths and bond angles were taken from previous work on similar compounds[7] and are listed in *Table 3*. The energies of the first- and second-order interactions (*Table 4*) were also generally taken from previous work[3]. One second-order interaction energy, E_ω, was modified from 1.41 kcal mol^{-1} to 0.3 kcal mol^{-1} in order to optimize agreement between results of calculations and experiment for these molecules.

The principal rotational isomers for the $O-CH_2$ and CH_2-CH_2 bonds were assigned torsion angles, ϕ, of 180°

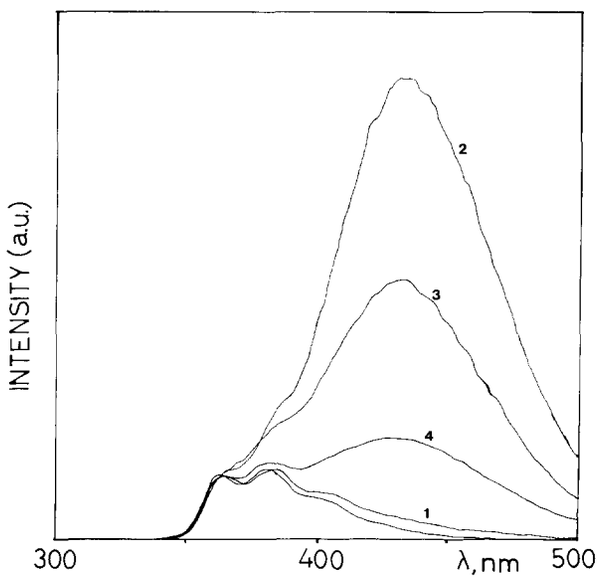

Figure 5 Emission spectra, normalized at 365 nm, for DMN and P_m, $m = 1-4$, in propanol at 25°C, using excitation at 296 nm. The unlabelled spectrum is for DMN, and the labelled spectra are for P_m with the indicated values of *m*

Table 2 Anisotropy of the fluorescence

	Emission (excitation), nm (nm)	
Compound	355(320)	375(336)
2MN	0.37	0.34
N1N	0.20	0.20
N2N	0.23	0.21
N3N	0.24	0.22
N4N	0.28	0.25
	359(336)	375(336)
DMN	0.40	0.40
P1	0.15	0.14
P2	0.16	0.15
P3	0.18	0.15
P4	0.19	0.16

Table 3 Bond lengths and bond angles

Bond	Length (Å)	Bonds	Angle (deg)
$C^{ar}-C^*$	1.47	$C^{ar}-C^*-O$	125
C^*-O	1.34	$C^{ar}-C^{ar}-C^*$	120
$O-CH_2$	1.44	$C^{ar}-C^{ar}-C^{ar}$	120
$C^{ar}-C^{ar}$	1.40	C^*-O-CH_2	113
CH_2-CH_2	1.53	$O-CH_2-CH_2$	110
		CH_2-O-CH_2	110

Table 4 Energies for first- and second-order interactions (from Mendicuti *et al.*[7])

Order	Atoms	Symbol	E (kcal mol^{-1})
First	$C^*-O-CH_2-CH_2$	E_σ	0.42
First	$O-CH_2-CH_2-O$	$E_{\sigma 1}$	−0.4
First	$CH_2-CH_2-O-CH_2$	$E_{\sigma 2}$	0.93
Second	$C^*\ldots O$	E_ω	0.3
Second	$CH_2\ldots O$	$E_{\omega 1}$	0.36
Second	$CH_2\ldots CH_2$	$E_{\omega 2}$	∞

Table 1 Values of I_D/I_M

	Solvents[a]						
Compound	DCE	Diox	EG	MeOH	POH	MMA	PMMA
N1N	0.14	0.086	0.18	0.30	0.30	0.053	0.068
N2N	0.61	0.32	0.58	1.22	1.39	0.32	0.062
N3N	0.31	0.19	0.32	0.86	0.96	0.12	0.059
N4N	0.20	0.12	0.25	0.54	0.60	0.096	0.045
P1	0.23	0.28	0.046	0.18	0.074	0.41	0.14
P2	2.13	1.44	1.04	3.17	2.24	2.39	0.45
P3	1.37	0.89	0.52	2.20	1.44	1.82	0.32
P4	1.52	1.08	0.23	1.05	0.56	1.31	0.31

[a] DCE = 1,2-dichloroethane, Diox = *p*-dioxane, EG = ethylene glycol, MeOH = methanol, POH = *n*-propanol, MMA = methyl methacrylate, PMMA = glassy poly(methyl methacrylate)

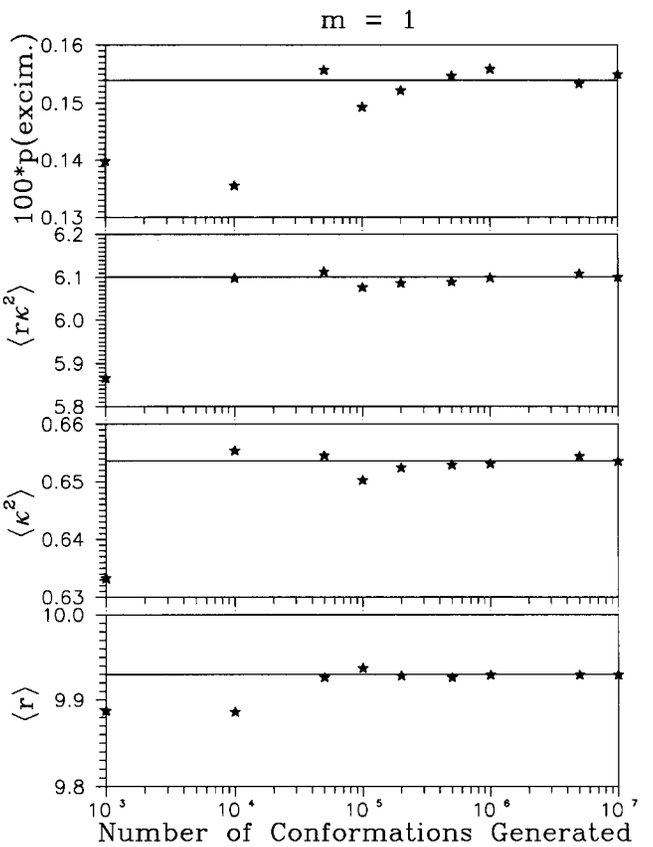

Figure 6 Convergence of the Monte-Carlo simulations (stars) to the exact results (horizontal lines) for $m=1$. Units for $\langle r\kappa^2\rangle$ and $\langle r\rangle$ are Å

(*trans*) and $\pm 60°$ (*gauche*$\pm$). Each principal rotational isomer is split into three states, of the same energy, with torsion angles separated by 20° and centred on the torsion angle for the principal rotational isomer. The nine states that result have ϕ of 180°, $\pm 160°$, $\pm 80°$, $\pm 60°$, and $\pm 40°$. There are also two rotational isomers at each C^{ar}–C* bond, equally weighted, with ϕ of 0° and 180°. The ester bond, C*–O, is maintained in the *trans* conformation, $\phi = 180°$. Thus the dimeric model compounds, NmN, have $2^2 3^{(3m)}$ conformations defined by the principal rotational isomers and $2^2 9^{(3m)}$ conformations when the splitting of each rotational isomer is introduced.

The conformations are examined for adherence to conditions for the formation of an approximation to a planar 'sandwich' by the two naphthalene rings in NmN. The criteria are $3.25\ \text{Å} < d < 4.0\ \text{Å}$, $0 < d_{XY} < 1.4\ \text{Å}$, and $0 < \psi < 40°$, where $d = (d_x^2 + d_y^2 + d_z^2)^{1/2}$ is the distance between the centres of mass of the two rings, d_{XY} is the lateral offset, and ψ is the angle between the normals to the planes of the rings. A Cartesian coordinate system having the origin at the centre of mass of one ring and Z axis perpendicular to that ring is used to compute the d_x, d_y and d_z coordinates.

By taking advantage of symmetry conditions and ignoring all conformations where every bond in $(O\text{–}CH_2\text{–}CH_2)_m\text{–}O$ is in the same principal rotational isomeric state (or the splitting of that state), the number of distinguishable conformations for $m=1$–3 is reduced to the point where they can all be examined with a reasonable amount of computer time. For $m=4$, however, that discrete enumeration would require an unreasonable amount of time (estimated at approximately 1 year on an SGI 4D/35 computer). Hence the analysis for N4N is achieved by a Monte-Carlo method that examines a representative subset of all conformations. The Monte-Carlo method was also applied to the smaller compounds, with $m=1$–3, to ensure that it correctly reproduces the results for the entire ensemble.

A random routine was employed to compute $3m+2$ random numbers that were used to determine the placement of each rotatable bond of the molecule (2 for the $C^*\text{–}C^{ar}$ bonds and $3m$ for the glycol residue), thus producing one conformation of the molecule. The procedure was repeated until the desired total number of conformations, N, was generated. All conformations thus produced were accepted and weighted with a Boltzmann exponential of their energies. Thus, the procedure is similar to the exact enumeration with the only difference of examining a predetermined number, N, of randomly generated conformations instead of analysing all the conformations allowed to the molecule. The performance of the random routine was checked by determining how many times each state of the rotatable bonds is generated. Typical results indicate that departures of *c.* 1% between expected and actually generated distributions are reached with $N \sim 10^4$ for the $C^*\text{–}C^{ar}$ bonds and $N \sim 10^5$ for the bonds on the glycol residue. Thus, each $C^*\text{–}C^{ar}$ bond is placed $N_0 = (1.00 \mp 0.01)N/2$ times in the conformation having $\phi = 0$ and $N\text{-}N_0$ times in $\phi = 180$ when $N > 10^4$. In a similar way, each of the nine states allowed to the bonds of the glycol residue appears to within $\sim 1\%$ of the theoretical expectation provided that $N > 10^5$.

The results from the Monte-Carlo calculations for $m=1$–4 are depicted in *Figures 6–9*, respectively. The top panel in each figure shows the probability for an

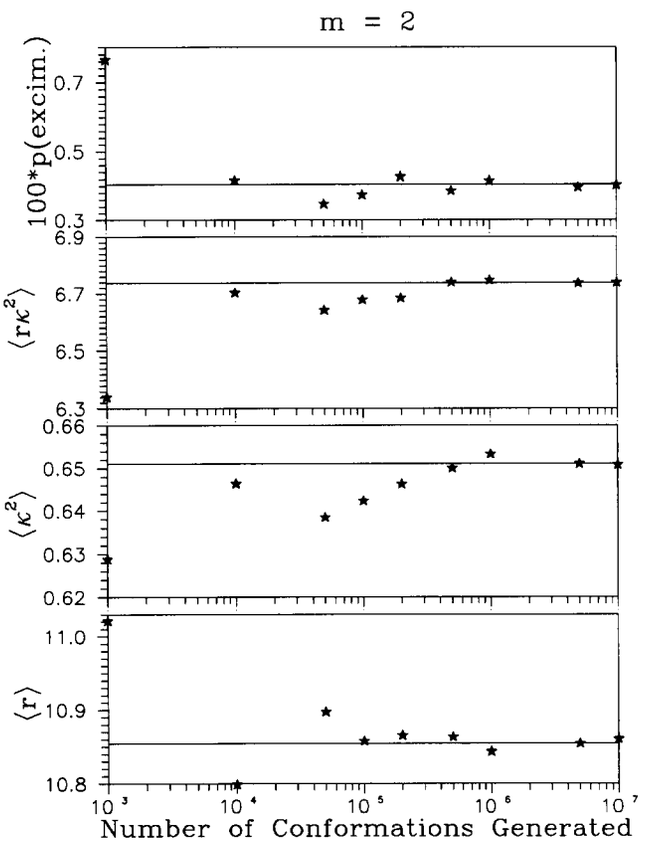

Figure 7 Convergence of the Monte-Carlo simulations (stars) to the exact results (horizontal lines) for $m=2$. Units for $\langle r\kappa^2\rangle$ and $\langle r\rangle$ are Å

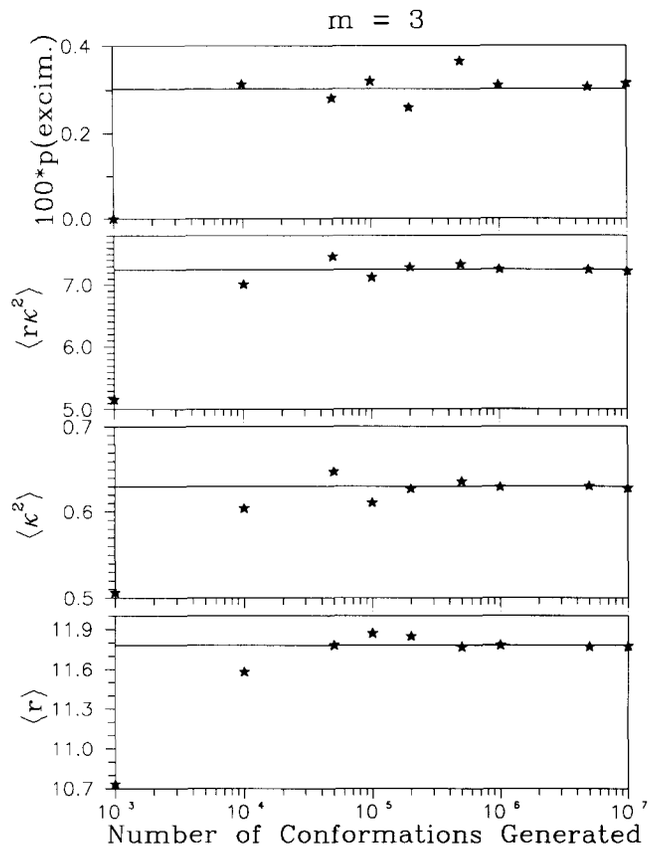

Figure 8 Convergence of the Monte-Carlo simulations (stars) to the exact results (horizontal lines) for $m=3$. Units for $\langle r\kappa^2\rangle$ and $\langle r\rangle$ are Å

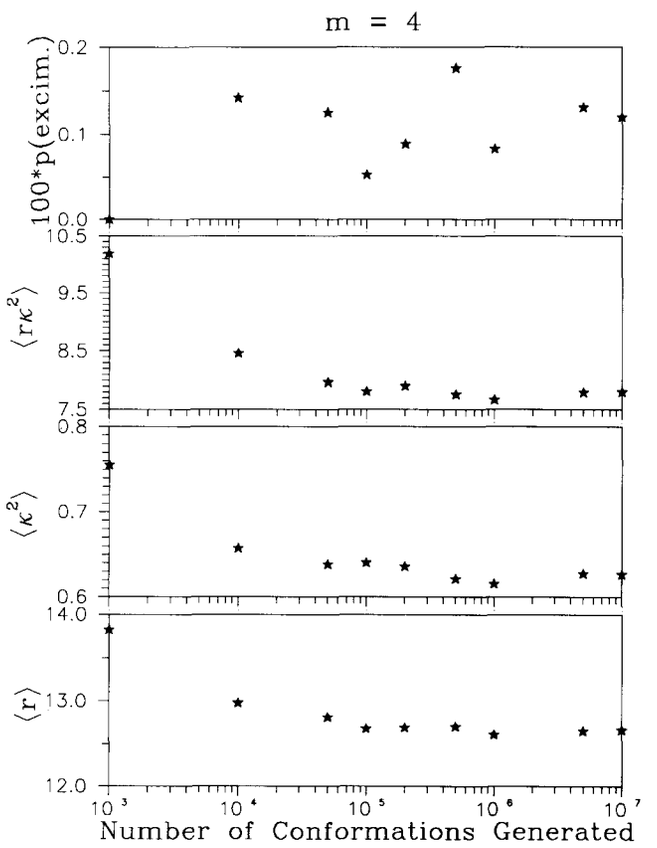

Figure 9 Convergence of the Monte-Carlo simulations to constant values for $m=4$. Units for $\langle r\kappa^2\rangle$ and $\langle r\rangle$ are Å

excimer-forming conformation (a conformation that satisfies the tolerances on d, d_{XY} and ψ), as a function of the number of chains generated in the Monte-Carlo simulation. The horizontal lines in *Figures 6–8* are the results from discrete enumeration. The Monte-Carlo calculations converge to the exact results in $\sim 10^6$ conformations when $m=1-3$. Results from discrete enumeration are not available at $m=4$, but those from the simulation appear to be approaching constant values at 10^7 conformations. The simulations predict the largest values of the probability for an excimer at $m=2$, which agrees with the spectra depicted in *Figures 2–5*. The next largest value is predicted (and observed) at $m=3$. The simulations predict smaller values (of comparable size) at $m=1$ and 4; experiments place the smaller value at $m=1$.

The simulations find that the average value of κ^2 is close to 2/3, which is the expectation for a system where there is a random distribution of the transition moments. The average separation increases from 9.93 Å at $m=1$ to 12.7 Å at $m=4$.

Figure 10 depicts the probability of finding the centre of masses of the two naphthalene rings separated by a distance not larger than R, i.e. if a sphere of radius R is centred on the centre of mass of one ring, p_R represents the probability of finding the centre of mass of the second ring inside this sphere. The orientational factor is introduced into the results by considering that the transition moments for excitation and emission are parallel and in the plane of the ring. *Figure 11* shows the ratio of $\kappa^2 p$ for all the conformations with R less the specified finite value to the value of $\kappa^2 p$ for all conformations. Similar trends are obtained for p_R and $\kappa^2 p$. According to *Figure 10*, values of R of 14.5 and 17.5 produce $p_R=1$ for $m=1$ and 2, respectively. Slightly larger values of R (21.5 and 24.5 Å, respectively) than those used in *Figure 10* are required for $p_R=1$ when m is 3 or 4. For $R<8.5$ Å the results of p_R show a maximum for $m=2$ and for $R\geqslant 98.5$ Å, the maximum value corresponds to $m=1$. The values of p_R exhibit a monotonic decrease as m increases for approximately 9 Å $< R <$ 14 Å.

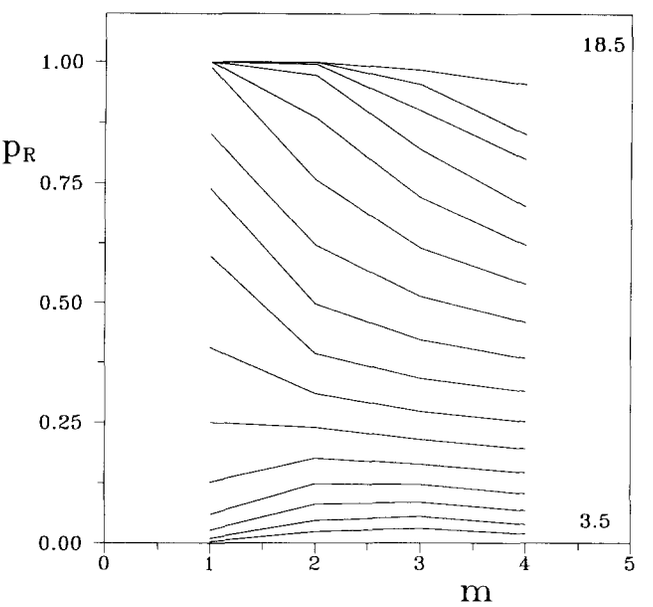

Figure 10 Dependence of p_R on R for 3.5 Å $< R <$ 18.5 Å. The values of R increase in units of 1 Å from the bottom curve to the top curve

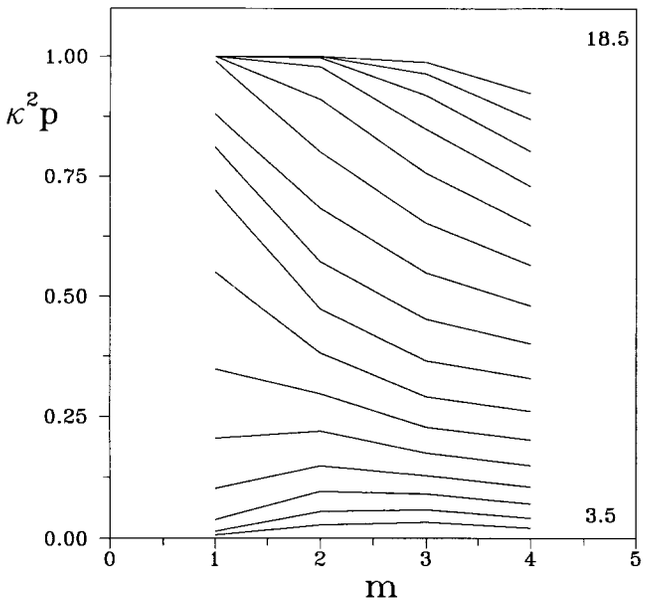

Figure 11 Dependence of $\kappa^2 p_R$ on R for 3.5 Å $< R <$ 18.5 Å. The values of R increase in units of 1 Å from the bottom curve to the top curve

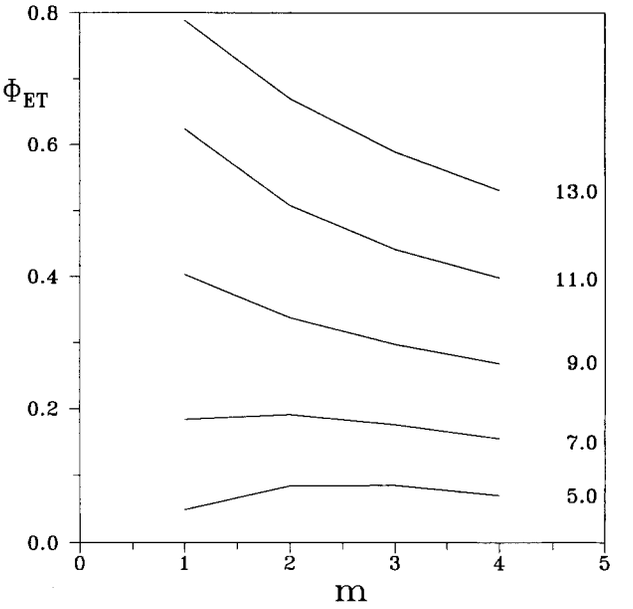

Figure 12 Estimates of the efficiency of Förster energy transfer with five assumptions about the value of R_0 for a random ensemble of chromophores

The efficiency of Förster transfer energy in *Figure 12* was obtained according to:

$$\Phi_{ET} = \Sigma_p (1 + R^6/R_0^6)^{-1} \quad (2)$$

where p is the probability of a conformation, R is the distance between centres of masses of the two naphthalene rings and R_0 is an assumed value for the Förster radius. The monotonic decrease of the efficiency with increasing m does not appear until R_0 reaches values as high as 9 Å. These results are consistent with prior estimates[3] of the values of R_0 for 2MN and DMN (12 and 14 Å) and with the experimental values of anisotropy as functions of m in rigid media. These values of R_0 imply efficient energy migration in the polymers.

ACKNOWLEDGEMENTS

This research was supported by the DGICYT through grant PB91-0166 and the National Science Foundation, DMR 89-15025.

REFERENCES

1 Guillet, J. 'Polymer Photochemistry and Photophysics', Cambridge University Press, Cambridge, 1985
2 Förster, Th. *Ann. Phys.* 1948, **2**, 55
3 Mendicuti, F., Saiz, E. and Mattice, W. L. *Polymer* (in press)
4 Makowski, M. P. and Mattice, W. L. *Polymer* (in press)
5 Patel, B., Mendicuti, F. and Mattice, W. L. *Polymer* 1990, **31**, 1877
6 Lakowicz, J. R. 'Principles of Fluorescence Spectroscopy', Plenum Press, New York, 1983, p. 126
7 Mendicuti, F., Viswanadhan, V. N. and Mattice, W. L. *Polymer* 1988, **29**, 875